ISSN 1027-4510, Journal of Surface Investigation: X-ray, Synchrotron and Neutron Techniques, 2023, Vol. 17, No. 3, pp. 724–729. © Pleiades Publishing, Ltd., 2023.
Russian Text © The Author(s), 2023, published in Poverkhnost', 2023, No. 6, pp. 107–112.

Comprehensive Study of the Local Atomic Structure of Promising Ti-Containing Compounds

I. K. Averkiev[a, *], O. R. Bakieva[a], and V. V. Kriventsov[b]

[a] *Udmurt Federal Research Center, Ural Branch, Russian Academy of Sciences, Izhevsk, 426008 Russia*

[b] *Boreskov Institute of Catalysis, Siberian Branch, Russian Academy of Sciences, Novosibirsk, 630090 Russia*

**e-mail: averkiev1997@mail.ru*

Received July 20, 2022; revised September 14, 2022; accepted September 14, 2022

Abstract—A comprehensive study of the local atomic structure of titanium compounds obtained by mechanical activation (Ti–Al–C, Ti_2AlC) and reference samples (Ti, TiH_2) using extended X-ray absorption fine structure (EXAFS) and extended electron energy loss fine structure (EXELFS) spectroscopy is carried out. An analysis of the local atomic structure of titanium hydride shows that the presence of hydrogen expands the crystal lattice and leads to a change in the parameters of the local atomic structure. This change is observed both in the EXAFS and EXELFS spectra. It is shown that after mechanical activation, the coordination numbers decrease, which may indicate the formation of a multiphase system. Further annealing leads to formation of the Ti_2AlC compound, which is confirmed by the results of model calculations.

Keywords: MAX phase, heat treatment, EXELFS spectroscopy, EXAFS spectroscopy, chemical bond length, local atomic structure

DOI: 10.1134/S1027451023030229

INTRODUCTION

The family of MAX-phase compounds includes layered ternary carbides and nitrides of 3*d* transition metals. The designation of the MAX phase is related to its chemical composition, where M is the 3*d* transition metal (Ti, Cr, Nb, V and others), A is the element of subgroups IIIA or IVA (Al, Si, In, Ge, Sn and others), and X is a light element, C and/or N [1]. Compounds of this class have a high hardness, melting point, corrosion resistance, and low expansion coefficient, which are characteristic of ceramic materials, but MAX phases have good electrical and thermal conductivity, which are characteristic of metals [2]. The combination of metallic and dielectric properties has ensured the use of MAX phases in various applications, including high-temperature structural materials and coatings [3, 4], corrosion-resistant coatings [5], catalysts [6], materials for solar-energy conversion [7] and storage of hydrogen [8], and precursors for two-dimensional carbides and nitrides [9]. Such a variety of properties is primarily due to a layered atomic structure with different types of chemical bonding and, as a consequence, anisotropy of the crystal lattice [10]. In these compounds, the localization of light elements can determine the final functional properties of the material.

Previously, the local atomic structure of MAX phases was studied mainly with respect to atoms of the 3*d* transition metal, without considering the local coordination of light elements. Extended X-ray absorption fine structure (EXAFS) spectroscopy is a classic method for studying the local atomic environment. This method is based on the detection of coherent scattering of photoelectrons by the local environment of the excited atom. High-intensity synchrotron radiation makes it possible to excite the internal *K* level of the metal atom; as a result, the analysis of EXAFS spectra provides information on the partial lengths of the metal chemical bond, thermal-dispersion parameters, and coordination numbers. The use of an electron beam makes it possible to quantify the parameters of the local environment of light elements by analyzing the extended electron energy loss fine structure (EXELFS) [11, 12]. The change in the energy of the incident electron beam makes it possible to obtain experimental EXELFS spectra beyond the *M* edges of excitation of the 3*d* metal and *K* edge of excitation of a light element (Li–F) at one depth of analysis. Thus, the purpose of this work is the comprehensive analysis of titanium compounds obtained by mechanical activation (Ti–Al–C, Ti_2AlC), and reference samples (Ti, TiH_2) using EXAFS and EXELFS spectroscopy and characterization of the local atomic structure with respect to metal and light element atoms.

MATERIALS AND METHODS

In this work, the test objects were titanium foil and titanium-hydride powder (99.4%) with particles no larger than 500 μm. The objects of study are a Ti–Al–C powder synthesized by mechanical activation, and the same powder after high-temperature annealing, which results in the formation of the Ti_2AlC phase [13]. The initial materials for mechanical activation were titanium, aluminum, and carbon powders. Petroleum ether was used as a modifying agent to avoid cold welding, sticking of the powder particles to the balls, and powder agglomeration during grinding. The particle size in the resulting powder did not exceed 5 μm. Subsequent annealing of the powders, which was carried out at 1000°C for 1 h in an argon atmosphere, is required for the formation of the Ti_2AlC phase.

The local atomic structure was studied by EXAFS and EXELFS spectroscopy. The experimental EXAFS spectra were obtained in the fluorescence-yield mode at the EXAFS experimental station of channel 8 of the VEPP-3 at the Center for Collective Use of the Siberian Center of Synchrotron and Terahertz Radiation, Novosibirsk. The VEPP-3 storage ring with an electron-beam energy of 2 GeV and an average current of 90 mA was used as the X-ray source. Radiation monochromatization was achieved using a split monoblock Si(111) monochromator crystal. The EXAFS spectra were obtained near the K absorption edges of Ti (E_b = 4966 eV). The step in measuring the EXAFS spectra was ~1.5 eV.

The EXAFS spectra were processed according to the standard procedure using the Viper and FEFF-7 programs [14–16]. The functions of the radial distribution of atoms were calculated from the normalized oscillating parts $k^2\chi(k)$ when using the inverse Fourier transform.

The experimental electron energy loss spectra were obtained in the geometry of the backscattering of secondary electrons by the sample surface on a JAMP-10S Auger spectrometer (JEOL) in a vacuum chamber with a residual pressure of no worse than 10^{-7} Pa. The presence of foreign impurities was monitored by Auger electron spectroscopy throughout the experiment; their concentration did not exceed 1 at %. The EXELFS spectra were obtained for the $M_{2,3}$ excitation edge of Ti (E_b = 34 eV) and K excitation edge of C (E_b = 284 eV) in the integrated mode (the beam brightness modulation (BBM) mode) at an energy of incident electrons of 900 eV, which corresponds to an analysis depth of 5 nm. The analysis of the extended fine structure of the electron energy loss spectra was carried out by the Fourier-transform method of the normalized oscillating parts of the spectrum.

Model systems were calculated, i.e., normalized oscillating parts of the spectra for compounds: Ti (sp. gr. $P6_3/mmc$, a = 2.950 Å, c = 4.685 Å), Ti_2AlC (sp. gr. $P6_3/mmc$, a = 3.058 Å, c = 13.652 Å), TiH_2 (sp. gr. $Fm\bar{3}m$, a = 4.454 Å), graphite (sp. gr. $P6_3/mmc$, a = 2.456 Å, c = 6.709 Å). Using the FEFF tables [16], the corresponding radial distribution functions were obtained.

RESULTS AND THEIR DISCUSSION

Figure 1 shows the Fourier images obtained from the EXAFS and EXELFS spectroscopy data for titanium foil in comparison with model calculations. The shape and position of the peaks show good qualitative and quantitative (Table 1) agreement of the results obtained using both synchrotron and electronic excitation. We note that the peaks obtained from the EXAFS spectroscopy data are broadened in comparison with model calculations, which may be due to the dispersion of the interatomic distances as a result of the thermal vibrations of atoms.

An analysis of the experimental EXAFS spectra of titanium hydride shows good agreement between the Ti–Ti interatomic distance and model calculations (Fig. 2a). In EXAFS spectroscopy, a hydrogen atom with a single electron does not make a significant contribution to backscattering and, as a result, there are no interatomic distances corresponding to Ti–H. This trend is observed both in model calculations and in the analysis of experimental spectra. However, compared with metallic titanium foil, the interatomic distances increase in all coordination spheres. This is due to the fact that hydrogen with a single electron does not make a significant contribution to backscattering, but behaves like an atom that expands the lattice. However, the lattice site occupied by hydrogen cannot be determined from the expansion of the lattice. Thus, the hydrogen atom, being between the atom that absorbed X-rays and the neighboring atom, at which the photoelectron was scattered, will change the phase shift and amplitude (the length of the chemical bond and the coordination number will change). Appropriate changes can be used to qualitatively determine the hydrogen content.

Analysis of the EXELFS spectra (Fig. 2b) shows that, in addition to the bonds related to titanium hydride, there is a Ti–O bond. This may be due to the depth of analysis upon electronic excitation, which did not exceed 5 nm; the analysis was carried out within several tens of atomic layers. Due to the natural adsorption of oxygen on the surface of the TiH_2 powder titanium oxides are inevitably formed [17, 18]. A similar pattern of surface-layer oxidation is also observed in the case of the powder after mechanical activation (Fig. 3b). It can be assumed that the differences in the parameters of the local atomic structure, determined from the experimental data and as a result of the corresponding model calculations, are associated with the formation of nonstoichiometric compounds of titanium, oxygen, and hydrogen [19].

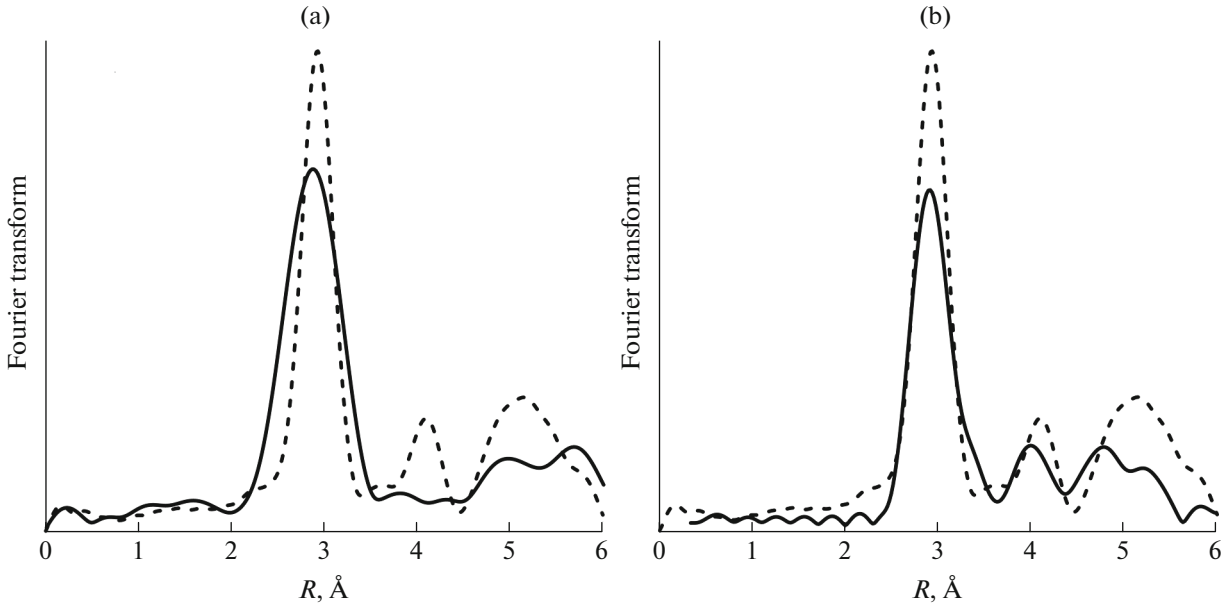

Fig. 1. Fourier transform of the normalized oscillating parts for titanium foil according to calculation results (dashed line) and experimental data (solid line): (a) EXAFS; (b) EXELFS.

Analysis of the EXAFS spectra of the powder after mechanical activation (Fig. 3a) shows the interatomic distances corresponding to pairs of Ti–C, Ti–Ti, and Ti–Al atoms. The differences from the corresponding model calculation can be associated with the formation of particles of the Ti–Al–C type without the formation of chemical bonds between elements as a result of mechanical activation [19].

Analysis of the EXELFS spectra obtained upon excitation of the *K* edge of absorption of carbon also allows one to determine the parameters of the Ti–C bond. The backscattering amplitude calculated for the excitation of a titanium atom is almost two times smaller than the amplitude calculated for a carbon atom (Fig. 4). That is, the contribution to the oscillating structure of the energy-loss spectra of electrons

Table 1. Model and experimental values of the parameters of the local atomic environment of titanium and carbon (chemical-bond length *R* (±0.10 Å), coordination number *N* (±5%))

Samples		*R*, Å			*N*		
		EXAFS	EXELFS	model	EXAFS	EXELFS	model
Ti	Ti–Ti	2.86	2.89	2.93	11.9	4.7	12.0
TiH_2	Ti–H/O	–	1.84	1.92	–	2.1	8.0
	Ti–Ti	3.13	2.96	3.15	11.8	8.9	12.0
Powder after mechanical activation	Ti–C/O	1.94	1.78	2.11	8.7	5.9	6.0
	Ti–Ti	2.95	2.94	3.07	2.2	1.7	6.0
	C–C (graphite)	–	1.46	1.41	–	1.7	6.0
	C–Ti	–	2.02	2.05	–	5.1	6.0
	C–C	–	3.10	3.06	–	3.6	6.0
Powder after annealing (Ti_2AlC)	Ti–C	2.15	1.90	2.11	3.2	8.3	6.0
	Ti–Ti	3.03	2.74	3.07	5.7	4.5	6.0
	Ti–Al	4.14	4.17	3.72	6.2	3.4	6.0
	C–C (graphite)	–	1.44	1.41	–	5.9	6.0
	C–Ti	–	2.08	2.05	–	3.8	6.0
	C–C	–	3.22	3.06	–	2.4	6.0

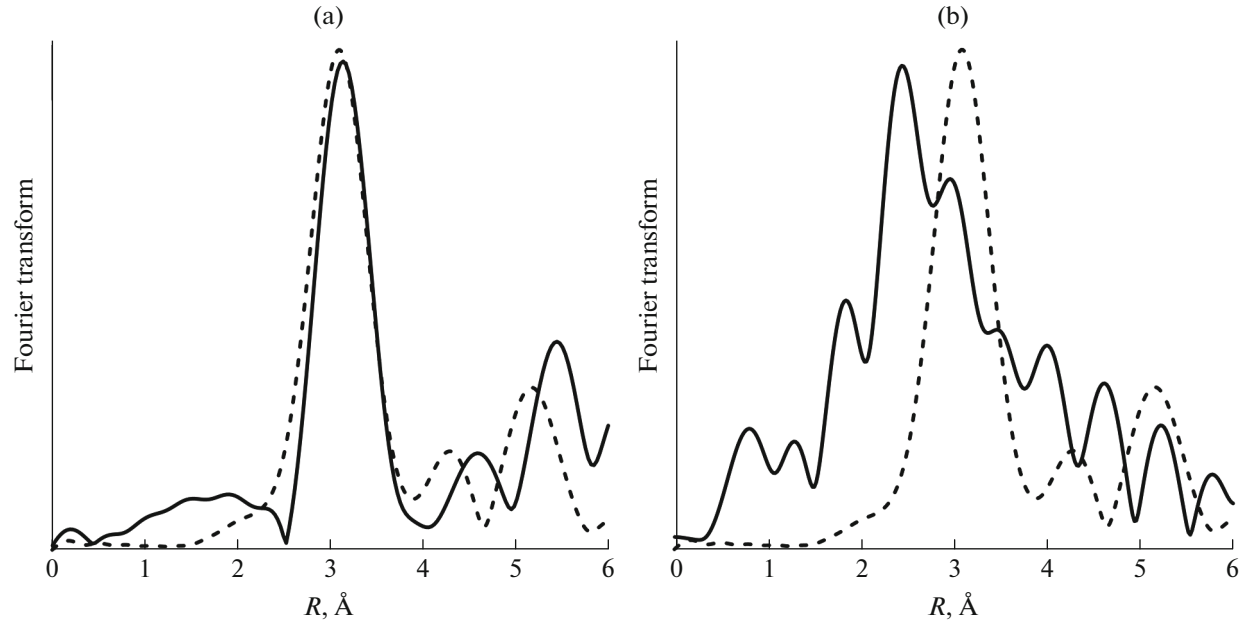

Fig. 2. Fourier transform of normalized oscillating parts for titanium-hydride powder according to calculation results (dashed line) and experimental data (solid line): (a) EXAFS (corrected for the phase shift); (b) EXELFS.

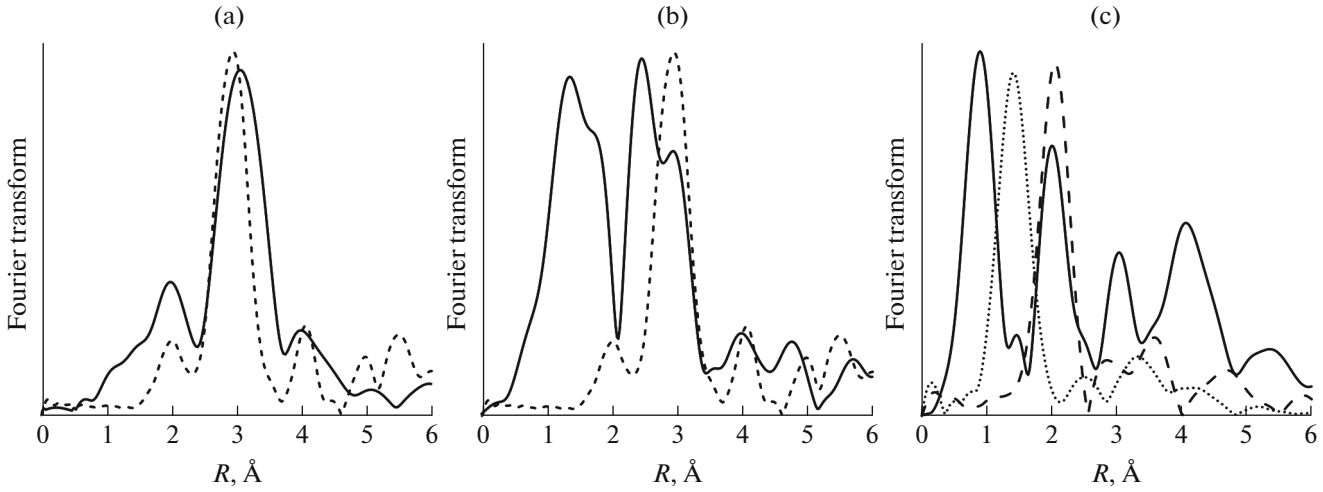

Fig. 3. Fourier transform of the normalized oscillating parts for the powder after mechanical activation according to the calculation results for the Ti_2AlC compound (dashed line), graphite (dashed line) and experimental data (solid line): (a) EXAFS, *K* absorption edge of Ti; (b) EXELFS, $M_{2,3}$ excitation edge of Ti; (c) EXELFS, *K* excitation edge of C.

from scattering at carbon atoms will be greater than from scattering at titanium atoms. This explains some differences in the results obtained from the experimental EXELFS spectra for the $M_{2,3}$ titanium excitation edge and *K* carbon excitation edge (Table 1).

The result of analysis of the EXELFS spectra for the *K* edge of excitation of carbon is shown in Fig. 3c in comparison with the model calculations for graphite and the Ti_2AlC compound. Good agreement between the experimental data and model calculations is observed. It can be noted that the superposition of the Fourier transforms of graphite and Ti_2AlC describes asymmetric peaks that are the sum of several interatomic distances. The intense peak at 1 Å is probably an artifact of experimental data processing and has no physical meaning.

As a result of annealing of the mechanically activated powder, the compound Ti_2AlC, which is confirmed by the good agreement between the parameters of the local atomic structure obtained from the

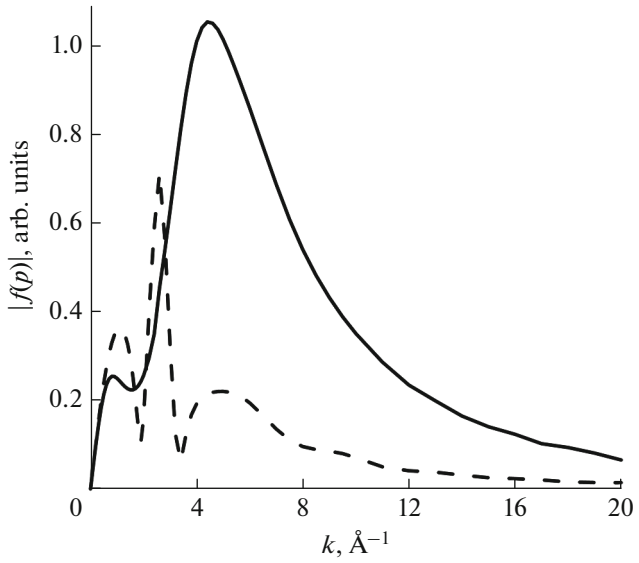

Fig. 4. Backscattering amplitudes for the $M_{2,3}$ excitation edge of titanium (dashed line) and the K excitation edge of carbon (solid line).

EXAFS data and as a result of model calculations (Fig. 5a, Table 1). Analysis of the EXELFS spectra for the $M_{2,3}$ titanium excitation edge also shows good agreement with the model calculations; however, it has the effect of oxidation of the surface of the Ti_2AlC compound [20, 21] and the formation of Ti–O interatomic bonds ~2 Å long (Fig. 5b). Analysis of the EXELFS spectra for the K edge of the excitation of carbon (Fig. 5c) showed that, after heat treatment, the coordination numbers increase and a peak appears at a distance of 1.44 Å, which can be attributed to the C–C distance in graphite. This indicates that the graphitization of carbon occurs as a result of powder annealing.

CONCLUSIONS

A study of the local atomic structure of titanium powders obtained by mechanical activation followed by annealing (Ti–Al–C, Ti_2AlC), and reference samples (Ti, TiH_2) using EXAFS and EXELFS spectroscopy was carried out. An analysis of the local atomic structure of titanium hydride showed that the introduction of hydrogen expands the crystal lattice: there is an increase in the interatomic distances in all coordination spheres compared to the distances in metallic titanium. This change is observed in the EXAFS and EXELFS spectra. It has been established that after mechanical activation, the coordination numbers decrease, which may indicate the formation of a multiphase system. Further annealing leads to the formation of the Ti_2AlC compound, which is confirmed by the results of model calculations.

ACKNOWLEDGMENTS

This work was supported by the Ministry of Science and Higher Education of the Russian Federation (Agreement no. 075-15-2022-263). The experiments were performed using large-scale research facilities "EXAFS spectroscopy beamline". The studies were carried out using the equipment of the Center for Collective Use "Center for Physical and Physico-Chemical Methods of Analysis, Study of the Properties and Characteristics of Surfaces, Nanostructures, Materials and Products" Udmurt Federal Research Center, Ural Branch, Russian Academy of Sciences. The study was performed at the Shared Research Center SSTRC on the basis of the VEPP-4-VEPP-2000 complex at the Budker

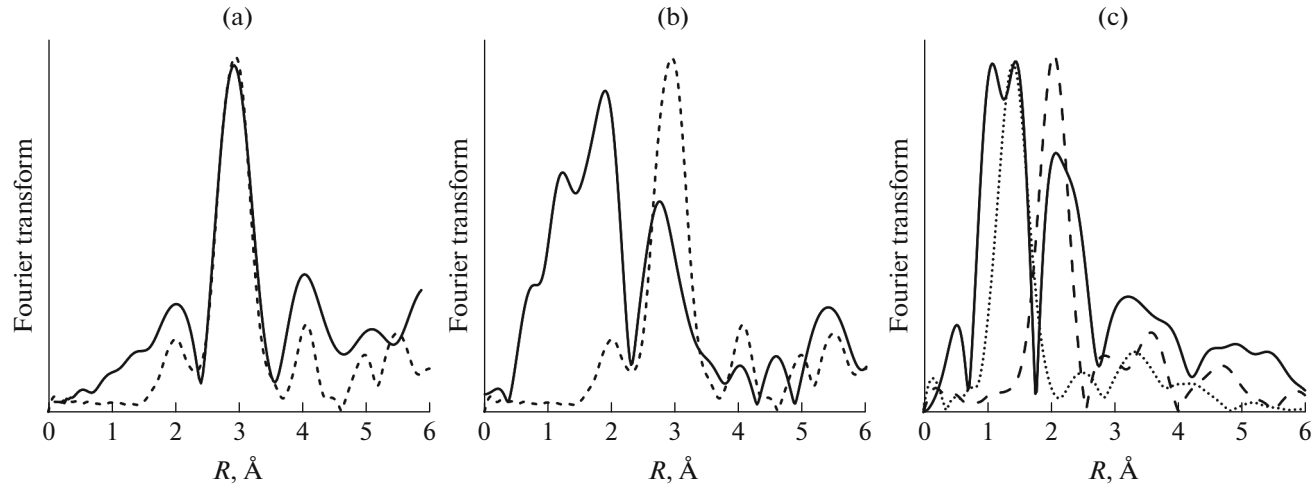

Fig. 5. Fourier transform of the normalized oscillating parts for the powder after annealing according to the calculation results for the Ti_2AlC compound (dashed line), graphite (dashed line) and experimental data (solid line: (a) EXAFS, K absorption edge of Ti; (b) EXELFS, $M_{2,3}$ excitation edge of Ti; (c) EXELFS, K excitation edge of C.

Institute of Nuclear Physicss, Siberian Branch, Russian Academy of Sciences.

CONFLICT OF INTEREST

The authors declare that they have no conflicts of interest.

REFERENCES

1. M. Sokol, V. Natu, S. Kota, and M. W. Barsoum, Trends Chem. **1**, 210 (2019). https://doi.org/10.1016/j.trechm.2019.02.016
2. M. W. Barsoum, Prog. Solid State Chem. **28**, 201 (2000). https://doi.org/10.1016/S0079-6786(00)00006-6
3. J. L. Smialek, Metall. Mater. Trans. A **49**, 782 (2018). https://doi.org/10.1007/s11661-017-4346-9
4. J. Gonzalez-Julian, G. Mauer, D. Sebold, D. E. Mack, and R. Vassen, J. Am. Ceram. Soc. **103**, 2362 (2020). https://doi.org/10.1111/jace.16935
5. Z. Wang, G. Ma, Z. Li, et al., Corros. Sci. **192**, 109788 (2021). https://doi.org/10.1016/j.corsci.2021.109788
6. I. M. Chirica, A. G. Mirea, S. Neatu, et al., J. Mater. Chem. A **9**, 19589 (2021). https://doi.org/10.1039/D1TA04097A
7. J. Sarwar, T. Shrouf, A. Srinivasa, et al., Sol. Energy Mater. Sol. Cells **182**, 76 (2018). https://doi.org/10.1016/j.solmat.2018.03.018
8. A. M. Lakhnik, I. M. Kirian, and A. D. Rud, Int. J. Hydrogen Energy **47**, 7274 (2022). https://doi.org/10.1016/j.ijhydene.2021.02.081
9. M. Naguib, M. Kurtoglu, V. Presser, et al., Adv. Mater. **23**, 4248 (2011). https://doi.org/10.1002/adma.201102306
10. M. Magnuson and M. Mattesini, Thin Solid Films **621**, 108 (2017). https://doi.org/10.1016/j.tsf.2016.11.005
11. O. R. Bakieva and O. M. Nemtsova, J. Electron Spectrosc. **222**, 15 (2018). https://doi.org/10.1016/j.elspec.2017.10.004
12. O. R. Bakieva, O. M. Nemtsova, and D. V. Surnin, J. Surf. Invest.: X-ray, Synchrotron Neutron Tech. **9**, 1039 (2015). https://doi.org/10.1134/S1027451015030180
13. M. A. Eryomina, S. F. Lomayeva, and S. L. Demakov, Mater. Chem. Phys. **273**, 125114 (2021). https://doi.org/10.1016/j.matchemphys.2021.125114
14. D. I. Kochubei, *EXAFS Spectroscopy in Catalysis* (Nauka, Novosibirsk, 1992) [in Russian].
15. K. V. Klementiev, Code VIPER for Windows. http://www.desy.de/_klmn/viper.html.
16. J. J. Rehr, FEFF Project. https://feff.phys.washington.edu/feffproject-feff.html.
17. C. Wang, Y. Zhang, Y. Wei, et al., Powder Technol. **302**, 423 (2016). https://doi.org/10.1016/j.powtec.2016.09.005
18. M. B. Novikova and A. M. Ponomarenko, Metal Sci. Heat Treat. **50**, 355 (2008). https://doi.org/10.1007/s11041-008-9072-x
19. I. K. Averkiev and O. R. Bakieva, J. Surf. Invest.: X-ray, Synchrotron Neutron Tech. **16**, 734 (2022). https://doi.org/10.1134/S1027451022030041
20. M. Dahlqvist, B. Alling, I. A. Abrikosov, et al., Phys. Rev. B **81**, 024111 (2010). https://doi.org/10.1103/physrevb.81.024111
21. J. R. Nelson, R. J. Needs, and C. J. Pickard, Phys. Rev. Mater. **5**, 123801 (2021). https://doi.org/10.1103/PhysRevMaterials.5.123801